

THE TEMPORAL AND GEOGRAPHIC EXTENT OF COLD TRAPPING REGIONS AT THE NORTH AND SOUTH POLE OF THE MOON: IMPLICATIONS FOR VOLATILE TRANSPORT AND THE SEASONALITY OF POLAR FROST DISTRIBUTION AND ABUNDANCE J.L. Kloos¹, J.E. Moores¹, J. Sangha¹, T.G. Nguyen¹, N. Schorghofer², ¹Centre for Research in Earth and Space Sciences, York University, Toronto, ON, Canada, ²Planetary Science Institute, Tucson, AZ, USA; jlkloos@yorku.ca

Introduction: Water ice deposits within lunar permanently shadowed regions (PSRs) remain important targets for study given their high value for science and exploration. Orbital mapping has revealed distinct trends in the geographic distribution of water and its derivatives – such as the pole-ward increase in hydrogen within the upper meter of regolith and surficial PSR frost abundance [1, 2] – which may be explained through a combination of loss/burial mechanisms (i.e. sublimation, sputtering, impact gardening) as well as patterns in transport and delivery to PSRs.

In this work, we perform Monte Carlo simulations of water transport in a collisionless setting to understand how water may be delivered to known PSRs at the north and south pole, and therefore assess the role that delivery may play in explaining the geographic trends observed from orbital data. Additionally, we utilize Lunar Orbiter Laser Altimeter (LOLA) digital elevation models (DEM) to model the polar illumination over the course of one draconic year (346.6 days) in order to identify regions at the surface that may act as temporary cold traps due to seasonal topographic shadowing owing to the small lunar obliquity ($< 1.59^\circ$). We assess the temporal and geographic extent of cold trapping regions at the north and south pole over the course of one lunar year, and explore their implications for the seasonality of polar frost distribution and abundance.

Monte Carlo Model: The Monte Carlo simulation used in this work was developed based on the work of Schorghofer [3] and Moores [4], however a few notable modifications have been made. Surface temperatures are modelled by implementing the Crank-Nicolson method to the one-dimensional heat equation using a 1-hr time step. Solar irradiance is determined as a function of latitude and longitude by computing the sub-solar point from a lunar fixed reference frame using the DE 421 lunar ephemeris at each time step (ignoring topography). To model the effects of seasonal temperature variation on volatile transport, twelve global temperature maps were produced that span one draconic year, beginning 29 July 2018 at the northern vernal equinox and ending on 9 July 2019. Each temperature map is spaced approximately 29 days apart, and is used to model the transport and trapping of water at a specific period of of the lunar year.

Each simulation begins with the production of individual H_2O molecules, hereby referred to as particles, onto the lunar surface. The generation of a particle initiates

the simulation wherein each particle is tracked in space and time until becoming trapped within a PSR or lost to the system through photolysis or escape. Particles are given random initial positions based on a uniform probability distribution, and are assumed to reach thermal equilibrium with the surface instantaneously, taking on a temperature proportional to the latitude and local time for the season being analyzed. Particle trajectories are simulated in three dimensions using a fourth order Runge-Kutta scheme, where the lunar atmospheric density is assumed low enough so as to be non-collisional, and therefore particle trajectories are described by simple gas dynamics. Cold traps are implemented using altimetrically-derived illumination maps produced by Mazarico et al. [5]. These maps chart the location of PSRs out to $\pm 65^\circ$ latitude at 240 meters-per-pixel resolution.

Illumination Model: Due to the obliquity of the moon, seasonal cold traps are expected to form at the winter pole, which may act as temporary reservoirs for water and other volatiles. The extent and distribution of the seasonal cold traps will depend on the local topography and time of year. Polar regions of topographic high may lie perennially exposed to sunlight, however the expanse of cold-trapping area at the winter pole would reach a maximum near the winter solstice when the solar insolation reduced.

To identify seasonal cold traps, we model the polar illumination over the course of one lunar year (for the same study period above) using LOLA gridded DEMs. To determine the sky visibility, the horizon method is used to calculate the elevation of the local horizon for individual surface elements (defined here as one pixel or a $240 \times 240\text{m}$ region of the lunar surface) at latitudes pole-ward of 85°N and S. The solar elevation is computed using the DE 421 lunar ephemeris with a 1-hr time step, and is cross-referenced with the horizon coordinates to determine the fraction of the Sun's disk that is visible for all regions of interest. Using this procedure, we create maps that record the time of year, as well as the length of time, that regions poleward of 85°N and S spend in shadow. These maps are used to constrain the locations where water may be temporarily stored.

Monte Carlo Results: In total, 12 Monte Carlo simulations were conducted with each simulation containing 2 million particles. We show the results of these simulations for the south pole in Figure 1. Here, the color axis corresponds to the particle concentration, which is

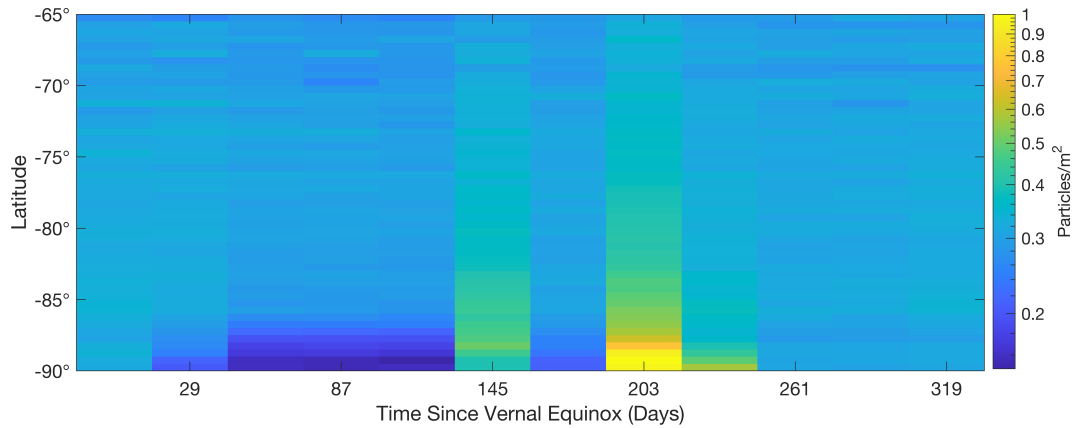


Figure 1: Geotemporal variations in volatile trapping within southern hemisphere PSRs spanning one draconic year. The color axis corresponds to the normalized particle concentration (particle count per unit PSR area) using a log scale. Data are binned using a 0.5° latitude bin spacing.

given by the quotient of the PSR particle count and the amount of PSR area within a 0.5° latitude bin. Vertical sections represent latitudinal profiles of particle concentration which are shown as a function of time.

As shown in Figure 1, temporal variations in PSR trapping manifest most strongly near the pole. At the equinox (time = 0), PSRs between $65^\circ - 90^\circ$ S exhibit a flat latitudinal distribution in concentration, with a marginal increase moving pole-ward. Approximately 29 days after the equinox, latitudes pole-ward of 88.5° S experience maximum temperatures of ~ 85 K, and thus water delivered to this region remains immobile until the arrival of warmer, spring temperatures. At time = 29 days, approximately 1.73% of particles released were seasonally trapped in the south. As winter approaches and the seasonal trapping area expands to include latitudes pole-ward of 87.5° S, the fraction of particles that are seasonally trapped increases to $\sim 3.53\%$ between time = 29 – 116 days.

The formation of seasonal cold traps acts to impede the transport of equatorial particles en route to the pole, leading to a reduction in the amount of water reaching the high-latitude PSRs when the seasonal traps are present. This can be clearly observed in Figure 1, where PSR concentrations nearest the pole are significantly reduced between time = 29 – 116 days. While the high-latitude PSRs may receive fewer particles when the solar insolation is reduced, the surrounding non-PSR polar terrain (pole-ward of $\pm 87.5^\circ$) may be temporarily enriched in seasonal water.

Water that is seasonally trapped will be released as the polar temperatures rise after the autumnal equinox. Water particles residing at the edge of the lunar polar circle ($\pm 87.5^\circ$) are the first to be liberated and enter the exosphere. The low polar temperatures at this time of year

produce relatively short hop distances (on the order of 100–150 km pole-ward of $\pm 80^\circ$ compared to > 200 km at the equator), which has two implications for liberated water: (1) the short flight time decreases the probability of loss, as only $\sim 1\%$ of all seasonally trapped particles were eventually destroyed or escaped, and (2) the decreased hop distance will serve to increase the amount of time, and the number of jumps that the particle will make at the pole. Given that this is the highest density region of PSRs at both poles, the vast majority of liberated water becomes trapped within a high-latitude PSR, while a minority migrate equator-ward and become trapped in a lower-latitude PSR. This can be seen in Figure 1 at time = 145 days, where a surge in PSR water concentration occurs due to the release of water trapped between $87.5^\circ - 88.5^\circ$ S and is even more evident at time = 203 days, when particles trapped between $88.5^\circ - 89.5^\circ$ S are released.

Conclusions: We find that seasonal temperature variations produce associated trends in the geographic accumulation of volatiles within lunar PSRs. The most pronounced seasonal trend in water transport and delivery occurs as a result of an extended cold trapping region at the winter pole which acts to impede the migration of water to high latitude regions. We map the location of seasonal cold traps where water may be seasonally stored; these results will be available by the time the conference commences.

References: [1] W. Feldman, et al. (2000) *Journal of Geophysical Research: Planets* 105(E2):4175. [2] P. O. Hayne, et al. (2015) *Icarus* 255:58. [3] N. Schorghofer (2014) *Geophysical Research Letters* 41(14):4888. [4] J. E. Moores (2016) *Journal of Geophysical Research: Planets* 121(1):46. [5] E. Mazarico, et al. (2011) *Icarus* 211(2):1066.